Regulation of Tumor Angiogenesis by Fastatin, the Fourth FAS1 Domain of βig-h3, via αvβ3 Integrin

Ju-Ock Nam, Ha-Won Jeong, Byung-Heon Lee, Rang-Woon Park, and In-San Kim

Cell and Matrix Biology National Research Laboratory, Department of Biochemistry, Kyungpook National University School of Medicine, Daegu, Korea

Abstract

We previously reported that the FAS1 domains of βig-h3 bear motifs that mediate endothelial cell adhesion and migration via interactions with αvβ3 integrin and regulate angiogenesis. In the present study, we show that the fourth FAS1 domain, designated fastatin, inhibits endothelial adhesion and migration, not only to βig-h3, but also fibronectin and vitronectin, in a RGD-dependent manner. Fastatin and other FAS1 domains suppress endothelial cell tube formation and *in vivo* neovascularization in a Matrigel plug assay. The antiangiogenic activity of fastatin is associated with antitumor activity in mouse tumor models. Fastatin additionally induces apoptosis in several cells expressing αvβ3 integrin, including endothelial cells. Binding of fastatin to αvβ3 integrin inhibits phosphorylation of focal adhesion kinase, Raf, extracellular signal-regulated kinase, Akt, and mammalian target of rapamycin. Fastatin is thus the first endogenous angiogenesis regulator identified that inhibits both endothelial cell migration and growth by binding to αvβ3 integrin. Our data suggest that FAS1 domains from all possible forms of the four human FAS1 family proteins are potential endogenous regulators for pathologic angiogenesis. Moreover, FAS1 domains such as fastatin may be developed into drugs for blocking tumor angiogenesis. (Cancer Res 2005; 65(10): 4153-61)

Introduction

βig-h3 is an extracellular matrix protein induced by the transforming growth factor-β in many cell types (1–4). Although the biological role is yet to be elucidated, a number of previous reports support its involvement in cell growth, differentiation, tumorigenesis, wound healing, and apoptosis (2–5). Moreover, the protein may play a role in the pathogenesis of some corneal, vascular, and renal diseases (6–9). The βig-h3 protein contains four homologous internal repeat domains similar to motifs in the *Drosophila* protein, fasciclin-I, and thus denoted "FAS1 domains." The FAS1 domains identified in the secretory and membrane proteins of many organisms, including mammals, insects, sea urchins, plants, yeast, and bacteria, contain highly conserved sequences (10). In humans, there are four proteins containing FAS1 domains, specifically, two secretory proteins, βig-h3 and periostin, and two membrane proteins, FEEL-1 and FEEL-2.

The FAS1 domain mediates cell adhesion and migration via interactions with integrins (11, 12). We previously reported that FAS1 domains of βig-h3 bear motifs interacting with integrins α3β1 (11) and αvβ5 (12). Recently, we showed that these domains additionally mediate endothelial cell adhesion and migration via the integrin, αvβ3, and the binding motif (YH18) comprising tyrosine, histidine, and flanking leucine/isoleucine residues inhibits angiogenesis (13). The YH18 peptide displays antiangiogenic activity at a high concentration of >100 μmol/L. In view of the finding that the YH18 motif is the minimal fragment mediating endothelial cell adhesion and migration while each FAS1 domain of βig-h3 is fully active, we assume that the FAS1 domain displays more potent antiangiogenic activity than the YH18 peptide.

Endostatin and tumstatin are two well-characterized endogenous angiogenesis regulators acting on integrins. Endostatin binds to α5β1 integrin, leading to inhibition of endothelial cell migration, but not growth, whereas tumstatin interacts with αvβ3 integrin in an RGD-independent manner, resulting in the blockage of endothelial cell growth but not migration (14). In the present study, we show that the fourth FAS1 domain of βig-h3, designated fastatin, inhibits endothelial cell migration to several matrix proteins in a RGD-dependent manner and has a potent antiangiogenic activity, both *in vitro* and *in vivo*. Exogenous administration of fastatin leads to significant antitumorigenic activity. Our data suggest that proteins containing FAS1 domains are potential endogenous regulators for pathologic angiogenesis, and FAS1 domains such as fastatin may be developed into drugs for blocking tumor angiogenesis.

Materials and Methods

DNA constructions and purifications. Bacterial expression plasmids for second and fourth FAS1 domain of human βig-h3, encoding amino acids 237 to 377 and 368 to 506 were generated by PCR (second FAS1 domain primer 5′-GATAAGATATCCTCCACCATCACCA-3′ and 5′-TCAAACTCGAGCTTGGCTGAGTCTG-3′; fourth FAS1 domain primer 5′-ATGGAGATATCGCTGACCCCCCCA-3′ and 5′-TCCTGCTCGAGGTTGGCTGGAGGC-3′) and cloned into the *Eco*RI and *Xho*I sites of pET29b (Novagen, Madison, WI), respectively. We named the fourth FAS1 domain of βig-h3 "fastatin." His-tagged recombinant proteins were expressed in BL21(DE3) cells, harvested, and purified using nickel/nitrilotriacetic acid/agarose column (Qiagen, Inc., Valencia, CA) as described previously (11). Endotoxin was removed by using polymixin B agarose (Pierce, Rockford, IL). Endotoxin was not detected by the *Limulus* Amebocyte Lysate test (Sigma Chemical Co., Louis, MO). To produce recombinant proteins for the third and seventh FAS1 domains of FEEL-2, each fragment of FEEL-2 cDNA, encoding amino acids 1030 to 1130 and 2356 to 2449 was generated by PCR (third FAS1 domain primer 5′-TTTACGGATCCACTGTCCTCGTGCCTTC-3′ and 5′-TTTAACTCGAGACTTTGTGGGACCAGC-3′; seventh FAS1 domain primer 5′-TTTAAGGATCCACCCTCTTTGTGCCAC-3′ and 5′-AAATACTCGAGACTGGGTGCTTTTAAAGGC-3′) and cloned into the *Bam*HI and *Xho*I sites of pET-43.1a (Novagen), named Nus-fas3 and Nus-fas7, respectively. The pET-43.1a is fused with the 491-amino-acid Nus Tag protein to improve the solubility of insoluble proteins. His-tagged recombinant Nus-fas3, Nus-fas7, and Nus proteins were expressed in BL21(DE3) cells, harvested, and purified using nickel-nitrilotriacetic acid-agarose column (Qiagen)

Requests for reprints: In-San Kim, Department of Biochemistry, Kyungpook National University School of Medicine, 101 Dongin-dong, Jung-gu, Daegu, 700-422, Korea. Phone: 82-53-420-4826; Fax: 82-53-422-1466; E-mail: iskim@knu.ac.kr.

according to the manufacturer's instruction. Endotoxin was removed by using polymixin B agarose (Pierce).

Cell culture. Primary human umbilical vein endothelial cells (HUVEC) and human embryonic kidney cells (HEK293) were cultured as described previously (13). Murine melanoma cells (B16F10) were cultured in RPMI 1640 containing 25 mmol/L HEPES with 10% fetal bovine serum (FBS). Human fibrosarcoma (HT1080), human glioblastoma (U87), human lung adenocarcinoma (A549), human colon adenocarcinoma (HT29), and human lung fibroblast (MRC5) cells were cultured at 37°C in 5% CO_2 in RPMI1640 (Life Technologies, Gaithersburg, MD) supplemented with 10% FBS.

Cell adhesion and migration assays. Cell adhesion assay was done as described previously (15). Briefly, flat-bottomed 96-well ELISA plates (Costar, Corning, Inc., NY) were incubated overnight at 4°C with 10 μg/mL of indicated protein and blocked for 1 hour at room temperature with PBS containing 2% bovine serum albumin (BSA). Fibronectin, vitronectin, and collagen were purchased from Promega (Madison, WI). Cells were suspended in medium at a density of 3×10^5 cells/mL, and 0.1 mL of the cell suspension was added to each well of the coated plates with or without the indicated concentration of fastatin or peptide. Synthetic peptides were purchased from Anygen (Kwangju, Korea). After incubation for 5 to 10 minutes at 37°C, unattached cells were removed by rinsing with PBS. Attached cells were then incubated for 1 hour at 37°C in 50 mmol/L citrated buffer (pH 5.0) containing 3.75 mmol/L *p*-nitrophenyl-*N*-acetyl-D-glycosamide and 0.25% Triton X-100. Enzyme activity was blocked by adding 50 mmol/L glycine buffer (pH 10.4) containing 5 mmol/L EDTA, and the absorbance was measured at 405 nm in a Bio-Rad model 550 microplate reader. Cell migration assay was done as described previously (13). Briefly, cell migration assays were done in transwell plates (8 μm pore size, Costar, Cambridge, MA). The undersurface of the membrane was coated with 10 μg/mL of indicated protein at 4°C and blocked for 1 hour at room temperature with PBS containing 2% BSA. Cells were suspended in medium at a density of 3×10^5 cells/mL, and 0.1 mL of the cell suspension was added to the upper compartment of the filter with or without the indicated concentration of fastatin. Cells were allowed to migrate for 6 to 8 hours at 37°C. Migration was terminated by removing the cells from the upper compartment of the filter with a cotton swab, and the filters were fixed with 8% glutaraldehyde and stained with crystal violet. The extent of cell migration was determined by light microscopy, and within each well, counting was done in nine randomly selected microscopic high power fields (×200).

***In vitro* and *in vivo* angiogenesis assays.** An *in vitro* endothelial tube formation was done as described previously (13). Matrigel (BD Bioscience, San Jose, CA) was added (100 μL) to each well of a 96-well plate and allowed to polymerize. Cells were suspended in medium at a density of 3×10^5 cells/mL, and 0.1 mL of the cell suspension was added to each well coated with Matrigel, together with or without the indicated recombinant proteins. Cells were incubated for 16 to 18 hours at 37°C. The cells were then photographed, and branch points from 4 to 6 high-power fields (×200) were counted and averaged. Each group consisted of three or four matrigels. An *in vivo* Matrigel plug assays were done as described previously (13). Briefly, 5- to 6-week-old male C57BL/6 mice were used. Matrigel (BD Bioscience) was mixed with 20 units/mL heparin, 0.15 μg/mL basic fibroblast growth (bFGF) factor (R&D Systems, Inc., McKinley, NE), and recombinant proteins. The Matrigel mixture (500 μL) was injected s.c., and after 7 days mice were sacrificed, and the Matrigel plugs were removed and fixed in 4% paraformaldehyde. The plugs were embedded in paraffin, sectioned, and H&E stained. Sections were examined by light microscopy, and the number of erythrocyte-filled blood vessels from 4 to 6 high-power fields (×200) were counted and averaged. Each group consisted of five or six Matrigel plugs.

Retroviral vector construction and transduction into the B16F10. Retroviral expression vector for human fastatin was constructed as follows. Fastatin cloned into the *Cla*I and *Bam*HI sites of the retroviral vector pLNCX (BD Biosciences) to generate pLNCX-fastatin. The retroviral vector constructs, pLNCX and pLNCX-fastatin, were individually transfected to packaging cell line PT67 using Lipofectin (Life Technologies). After transfection for 36 hours, supernatants were collected and filtered through 0.45-μm syringe filters. Filtered medium was supplemented with Polybrene to a final concentration of 8 μg/mL. Target cells, murine melanoma cells (B16F10), were infected by incubation with these supernatant for 6 hours at 37°C. After incubation, dishes were washed twice with PBS and RPMI 1640 containing 25 mmol/L HEPES with 10% FBS added. For selection, the medium contained 1 mg/mL active G418 (Life Technologies). The selected cells were collected and designated as pLNCX/B16F10 and fastatin/B16F10. The secreted fastatin was confirmed in the culture supernatant of fastatin/B16F10 cells by immunoblotting using a polyclonal antibody (4) specific for the fourth domain of βig-h3.

Antitumor assay. The above transfected melanoma cells (1×10^6 cells/0.1 mL), pLNCX/B16F10 and fastatin/B16F10, were injected s.c. into the flanks of C57BL/6 mice (5- to 6-week-old males). Each experimental group consisted of six to eight mice. Tumor sizes were measured with a Vernier caliper every 2 to 3 days, and volumes were calculated using the standard formula: $\text{width}^2 \times \text{length} \times 0.52$.

Male BALB/c nude mice (4-5 weeks old) were implanted with 1×10^6 B16F10 cells into the flank subcutis. Experimental groups were i.p. injected daily with fastatin at 9 or 18 mg/kg in a total volume of 0.1 mL PBS. The control group was given an equal volume of PBS each day. Each experimental group consisted of six to eight mice. Fastatin for injection was mixed with polymixin B-agarose (Sigma Chemical) for 2 hours at 4°C to remove endotoxin. Tumor sizes were measured using Vernier calipers every 2 to 3 days, and the volumes were calculated using the standard formula: $\text{width}^2 \times \text{length} \times 0.52$.

CD31 immunostaining. Intratumoral microvessel density (MVD) was analyzed on frozen sections of B16F10 tumor using a rat anti-mouse CD31 monoclonal antibody (PharMingen, San Diego, CA). Immunoperoxidase staining was done using the Vectastain avidin-biotin complex Elite reagent kit (Vector Laboratories, Burlingame, CA). Sections were counterstained with methyl green. MVD was assessed initially by scanning the tumor at low power, followed by identification of three areas at the tumor periphery containing the maximum number of discrete microvessels, and counting individual microvessels at a low magnification field (×40). Each group consisted of six or eight Matrigel plugs.

Proliferation assay. The measurement of viable cell numbers was carried out using the mitochondrial reduction activity assay (16). A suspension of cells (3,000 cells per well) was plated in a 96-well plate and cells were serum starved for 24 hours. The next day, fastatin was added and incubated for 48 hours and 3-(4,5-dimethylthiazol-2-yl)-2,5-diphenyltetrazolium bromide (MTT, Sigma Chemical) was added to each well. Cells were lysed with DMSO and quantified by the measurement of $A_{570\ nm}$ using an ELISA reader. The proliferation assay was carried out using the bromodeoxyuridine (BrdUrd) incorporation assay. To measure BrdUrd incorporation, cells were incubated on plates in the presence or absence of fastatin in M199 (HUVEC) or RPMI 1640 (MRC5) for containing 1% to 2% FBS, followed by BrdUrd (Oncogene Research Product, Boston, MA) for 6 hours in the culture incubator. BrdUrd uptake by the cells was detected using a Cell Proliferation Assay Kit (Oncogene Research Product).

Flow cytometric analysis. Cells were detached by gentle treatment with 0.25% trypsin, 0.05% EDTA in PBS, washed, and incubated for 1 hour at 4°C with antibodies to the αvβ3 (LM609). Cells were then incubated for 1 hour at 4°C with 10 μg/mL of the secondary antibody, goat anti-mouse immunoglobulin G conjugated with FITC (Santa Cruz Biotechnology, Inc., Santa Cruz, CA), and analyzed at 488 nm on the flow cytometer FACScalibur system (BD Biosciences) equipped with a 5-W laser.

Apoptosis assay. To assay apoptosis using FITC-Annexin V staining, cells were serum starved for 24 hours and incubated on plates in the presence of fastatin or tumor necrosis factor-α (TNF-α, 0.04 μg/mL) in M199 containing 2% FBS for 48 hours, followed by FITC-Annexin V (Santa Cruz Biotechnology) for 20 minutes in the dark. Washed cells were analyzed at 488 nm on the flow cytometer FACScalibur system (BD Biosciences) equipped with a 5-W laser. To measure caspase 3–like activity, HUVEC cells were plated at equal densities in 100-mm culture plates and either treated with fastatin or left untreated. Caspase 3–like enzymatic activity was detected using the EnzCheck Caspase-3 assay kit

(Molecular Probes, Inc., Eugene, OR). Each cell lysate was additionally tested in the presence of DEVD-CHO (10 μmol/L) to eliminate caspase 3–like activity.

Cell signaling experiment. Cells were serum starved for 24 hours and preincubated with or without fastatin, in the presence of 1% to 2% FBS for indicated time. Next, cells were lysed with modified radioimmunoprecipitation assay buffer [50 mmol/L Tri-HCl (pH 7.4); 1% NP40; 150 mmol/L NaCl; 1 mmol/L EDTA; 1 mmol/L phenylmethylsulfonyl fluoride; 1 mmol/L Na_3VO_4; and 5 mg/mL each of aprotinin, leupeptin, and pepstatin] on ice for 1 hour. The lysates were clarified by centrifugation (12,000 × *g* for 10 minutes at 4°C). Protein concentrations were determined using a Bio-Rad detergent-compatible protein assay kit (Bio-Rad, Hercules, CA) with BSA as a standard. For Western blot analysis, protein lysates were separated by electrophoresis on SDS-polyacrylamide gels. The gels were transferred onto polyvinylidene difluoride membranes and the blots were blocked with TBST (50 mmol/L Tris-HCl, 150 mmol/L NaCl, and 0.05% Tween 20) containing blocking reagents for 1 hour. The blots were incubated with primary antibodies for 16 hours at 4°C and washed thrice in TBST. The proteins were visualized with an enhanced chemiluminescence reagent (Amersham Pharmacia Biotech., Piscataway, NJ) and exposed to film. The following antibodies were used in this study: anti–phosphotyrosine 397 focal adhesion kinase (FAK), anti-FAK, anti–phosphoserine 338 Raf, anti-Raf, anti–phosphotyrosine 204 ERK, and anti-ERK antibodies from Santa Cruz Biotechnology, anti–phosphoserine 473 AKT, anti-AKT, anti–phosphoserine 2448 mammalian target of rapamycin (mTOR), and anti-mTOR antibodies from BD Transduction Laboratories (Lexington, KY).

Statistical analysis. All values are expressed as mean ± SE. The statistical significance of differential finding between experimental and control groups was determined by Student's *t* test. $P < 0.05$ was considered statistically significant and is indicated with an asterisk over the value.

Results

Fastatin inhibits angiogenesis, both *in vitro* and *in vivo*. To determine the potential antiangiogenic properties of fastatin, we initially measured its ability to inhibit endothelial cell adhesion and migration to extracellular matrix proteins. Fastatin induced dose-dependent inhibition of adhesion and migration to extracellular matrix proteins (Fig. 1*A-B*). Interestingly, fastatin strongly suppressed the adhesion and migration of endothelial cells to βig-h3, vitronectin, and fibronectin and weakly to collagen (Fig. 1*A-B*). Adhesion and migration of endothelial cells to βig-h3, vitronectin, and fibronectin were inhibited by the RGD peptide, whereas adhesion and migration to collagen (Fig. 1*C-D*) was not, suggesting that binding of fastatin to αvβ3 integrin is RGD dependent.

We examined the ability of fastatin to disrupt endothelial cell tube formation in Matrigel. Fastatin (5 and 10 μmol/L) inhibited endothelial tube formation in a dose-dependent manner (Fig. 2*A-B*). To confirm the antiangiogenic activity of fastatin *in vivo*, we measured the extent of blood vessel invasion into Matrigel plugs. Similar to the data obtained from the tube formation assay, the extent of blood vessel invasion was inhibited

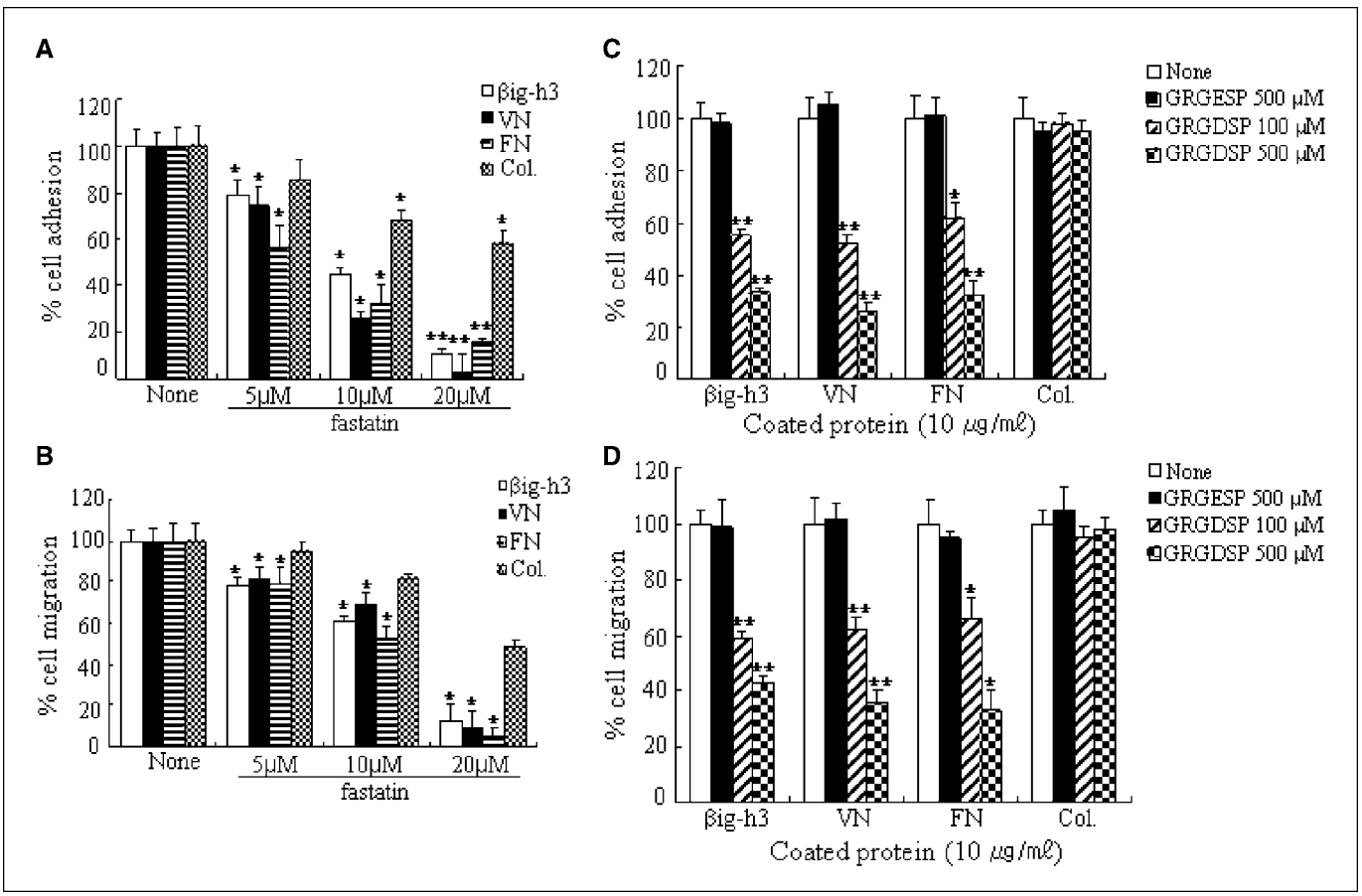

Figure 1. *In vitro* antiangiogenic activities of fastatin. *A-D,* adhesion and migration assay. *A-B,* fastatin was tested at a range of concentrations for its ability to inhibit endothelial cell adhesion and migration to βig-h3 (□), vitronectin (■), fibronectin (▤), or collagen (▨). *None,* background adhesion and migration in the absence of fastatin. *C-D,* RGD peptide was tested at a range of concentrations for its ability to inhibit endothelial cell adhesion and migration to βig-h3 (□), vitronectin (■), fibronectin (▨), or collagen (▩). *None,* background adhesion and migration in the absence of synthetic peptide. GRGESP is a control peptide. Cell migration was quantified by counting migrated cells in 9 high-power fields. ***, $P < 0.001$; **, $P < 0.01$; *, $P < 0.05$.

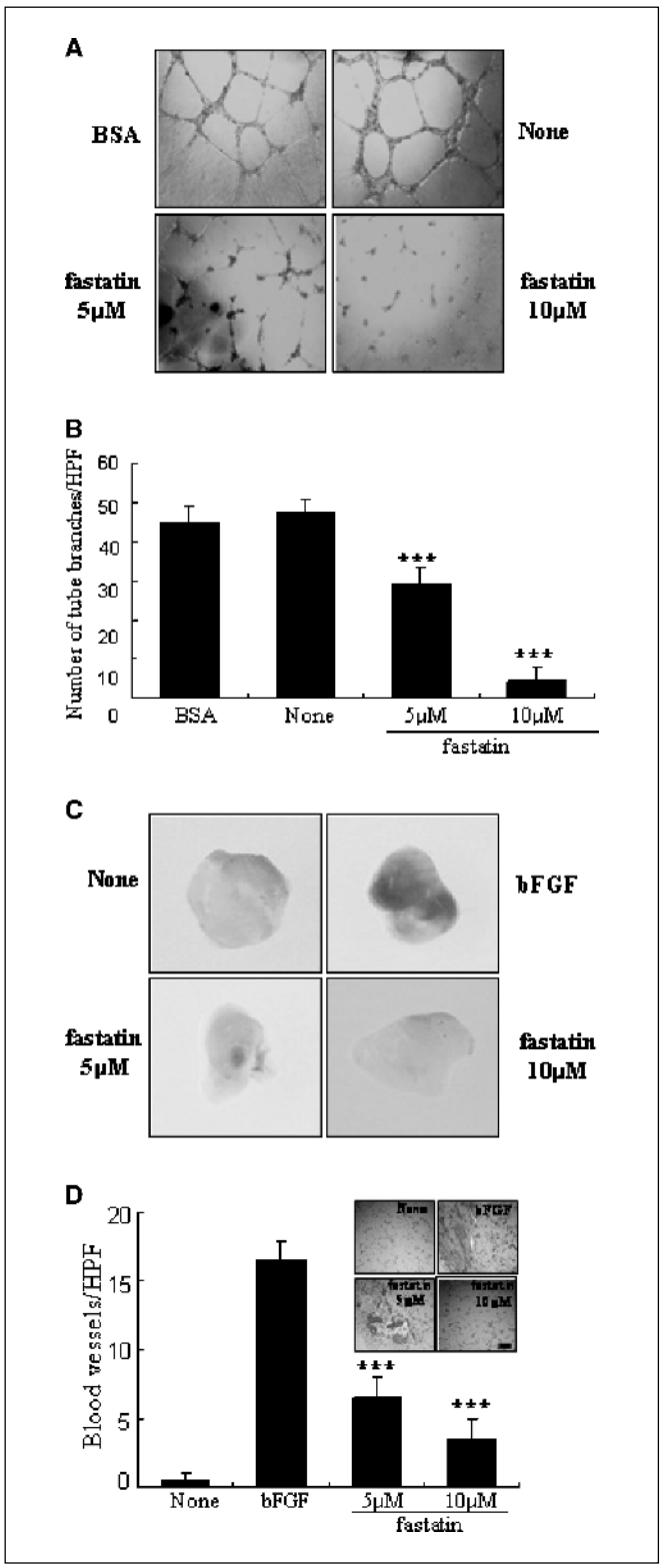

Figure 2. *In vitro* and *in vivo* antiangiogenic activities of fastatin. *A-B,* tube formation assay. *A,* cells were seeded on Matrigel in the absence or presence of fastatin (5 or 10 μmol/L) and photographed after 16 to 18 hours. *B,* quantitative analysis of the tube assay. *HPF,* high-power field (×200). *Columns,* means of triplicate wells; *bars,* ±SE. These experiments were repeated thrice. *Bar*, 100 μm. *C-D,* Matrigel plug assay. Fastatin (5 or 10 μmol/L) was mixed with Matrigel plus bFGF and injected into the flank of mouse. Sections of each Matrigel plug stained with H&E were examined by light microscopy (200× magnification). *Inset,* quantitative analysis of the Matrigel plug assay. ***, $P < 0.001$. *Bar*, 20 μm.

by 5 and 10 μmol/L fastatin. Fastatin (10 μmol/L) almost completely inhibited angiogenesis in a Matrigel plug assay (Fig. 2*C-D*). To determine whether other FAS1 domains similarly inhibit angiogenesis, we repeated the experiment with the second FAS1 domain of βig-h3 and the third and seventh FAS1 domains of FEEL-2. These FAS1 domains also inhibited endothelial tube formation and the second FAS1 domain of βig-h3 domain inhibited vascular invasion into the Matrigel plug (Fig. 3*A-C*).

Fastatin inhibits tumor growth. To analyze whether the antiangiogenic effect of fastatin inhibits tumor growth *in vivo*, B16F10 melanoma cells stably transfected with a retroviral vector encoding fastatin (fastatin/pLNCX) or an empty vector (pLNCX; Fig. 4*A*) were employed for *in vivo* tumor formation. Overexpression of fastatin itself did not affect B16F10 cell growth *in vitro* (Fig. 4*B*). However, fastatin-expressing cells did not form a detectable tumor up to 13 days of implantation. Following this time, we observed a slight increase in tumor size. In contrast, control tumor cells stably

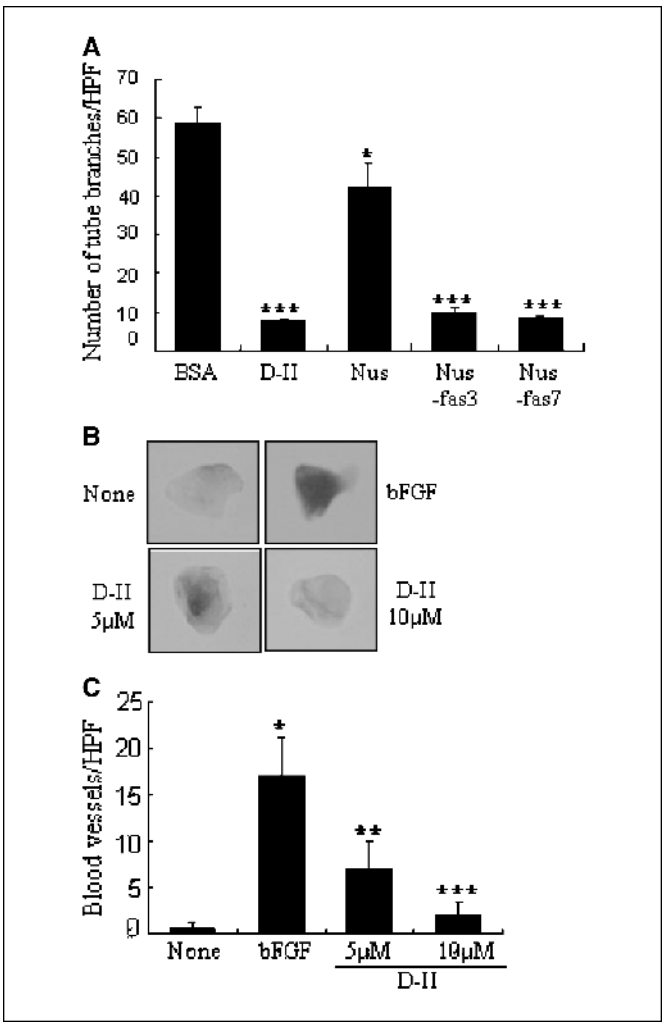

Figure 3. *In vitro* and *in vivo* antiangiogenic activities of other FAS1 domains. *A,* tube formation assay. Cells were seeded on Matrigel in the absence or presence of the Nus (10 μmol/L), second FAS1 domain of βig-h3 (D-II, 10 μmol/L), third FAS1 domain of FEEL2 (Nus-fas3, 10 μmol/L), or seventh FAS1 domain of FEEL2 (Nus-fas7, 10 μmol/L), and the number of tube branches were counted in a low-power field after 16 to 18 hours. *B,* Matrigel plug assay. The second FAS1 domain of βig-h3 (D-II) was mixed with Matrigel plus bFGF and injected into the flank of a mouse. After 7 days, Matrigel plugs were photographed. *C,* quantitative analysis of the Matrigel plug assay. *Columns,* means of five to six plugs/group; *bars,* ±SE. ***, $P < 0.001$; **, $P < 0.01$; *, $P < 0.05$.

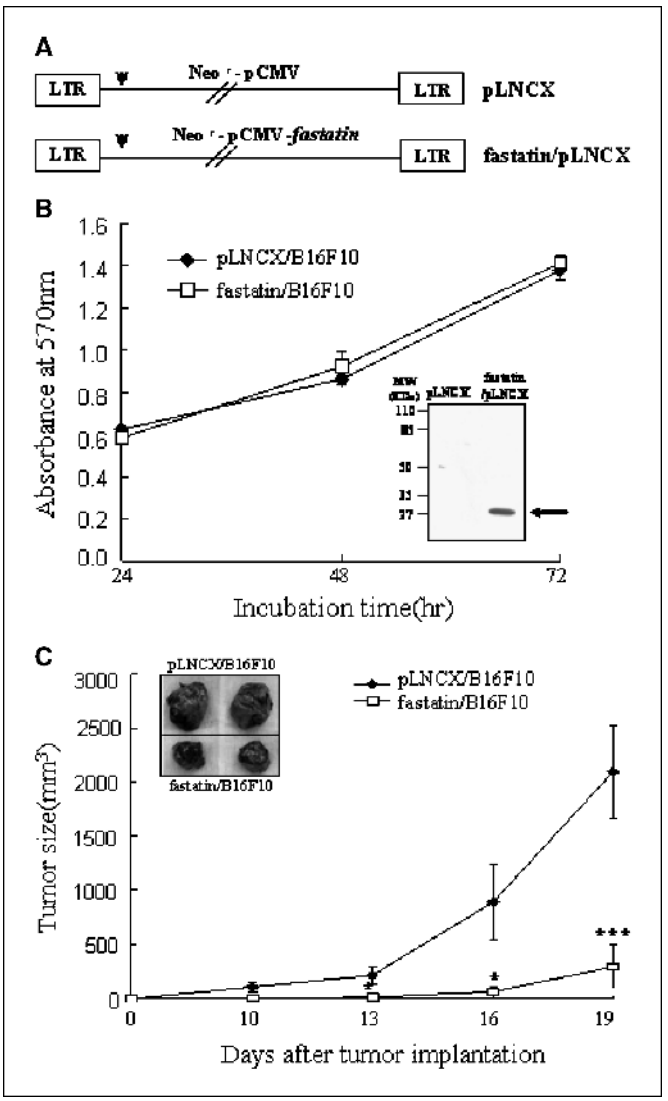

Figure 4. Fastatin inhibits tumor growth. *A,* preparation of retroviral vectors for fastatin expression. *B,* fastatin overexpression in melanoma cells does not affect cell growth *in vitro*. *Points,* means of three determinations ($n = 3$) by the MTT assay. No significant differences were observed between the mean $A_{570\ nm}$ values of pLNCX/B16F10 and fastatin/B16F10. *Inset,* expression of fastatin was analyzed in the cell supernatant by Western blot analysis with antibody specific for βig-h3. *C,* fastatin overexpression in melanoma cells inhibits tumor growth *in vivo*. Tumors of fastatin-expressing cells grow slower, compared with control tumors. *Inset,* tumor of fastatin-expressing cell (*bottom*) and control tumor (*top*), whole tumor tissue at 19 days of implantation. ***, $P < 0.001$; *, $P < 0.05$.

transfected with empty vector showed a dramatic increase in tumor size after 13 days of cell implantation (Fig. 4*C*). Next, we used a BALB/c nude mouse tumor model to determine whether exogenous fastatin inhibits tumor formation. We implanted B16F10 melanoma cells s.c. into the flanks of nude mice and monitored tumor growth and neovascularization after systemic treatment with exogenous fastatin. Protein (9 or 18 mg/kg) was i.p. injected everyday from 7 days after tumor cell implantation. Fastatin significantly inhibited tumor growth, compared with control (Fig. 5*A*). To determine whether the reduced size of fastatin-treated tumors coincides with reduced neovascularization, we used eight representative fastatin-treated or PBS-treated tumors to quantify the density of microvessels after immunostaining with CD31 antibody. This reduced size of fastatin-treated tumors was consistent with a decrease in CD31-positive microvessels (Fig. 5*B-C*). No differences in body weight were observed between the groups (data not shown).

Fastatin induces endothelial cell apoptosis via αvβ3 integrin. The αvβ3 integrin is required, not only to mediate endothelial cell adhesion and migration, but also for proliferation and survival. Accordingly, in subsequent experiments, we examined whether fastatin affects endothelial cell growth and survival. Fastatin significantly inhibited the serum-stimulated proliferation of HUVEC, HT1080, and U87 in a dose-dependent manner but not that of A549, MRC5, and HT29 (Fig. 6*A-B*). Similar results were obtained using the BrdUrd incorporation assay with HUVEC but not that of MRC5

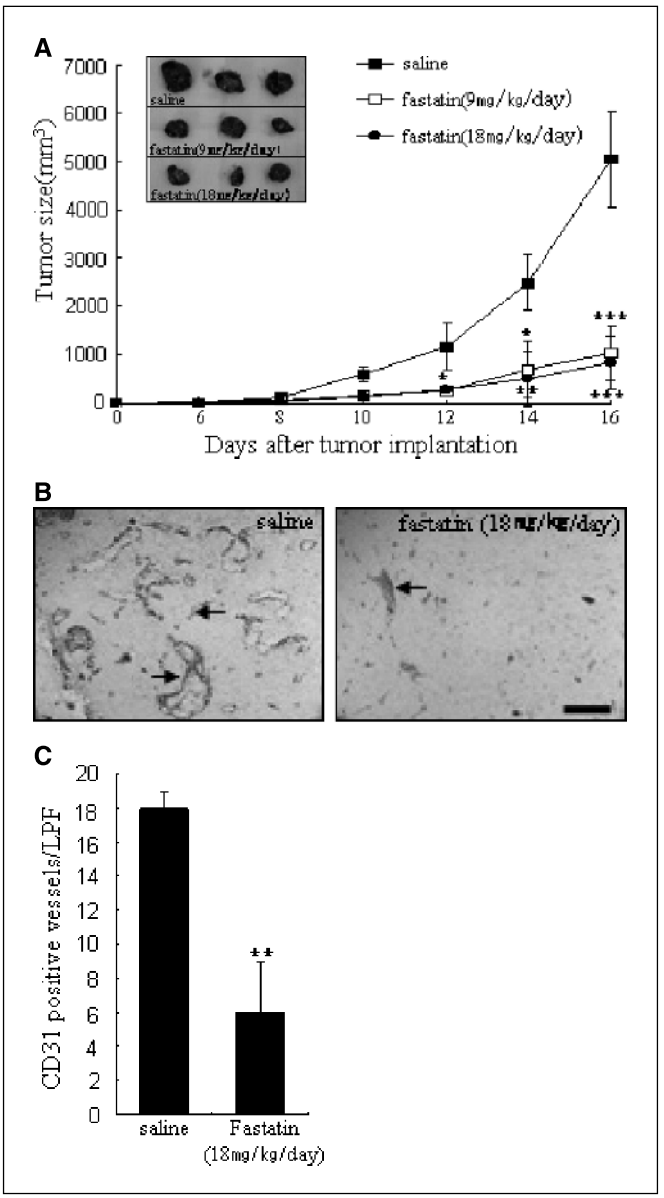

Figure 5. Fastatin inhibits tumor growth in a B16F10 tumor model. *A,* daily i.p. injections of human fastatin (9 or 18 mg per kg per day) inhibited the growth of B16F10 tumor, compared with the PBS control. *Inset,* i.p. injections of saline (*top*), human fastatin (9 mg per kg per day, *middle*), and human fastatin (18 mg per kg per day, *bottom*) whole tumor tissue at 16 days of implantation. *B-C,* blood vessel quantification in fastatin-treated tumors (18 mg per kg per day). Frozen sections (4 μm) from tumor tissue were stained with anti-CD31 antibody, and the number of CD31-positive blood vessels were counted. *LPF,* low-power field (×40). *Arrow,* CD31-positive blood vessel. *Points,* means of six to eight mice; *bars,* ±SE. ***, $P < 0.001$; **, $P < 0.01$; *, $P < 0.05$. *Bar*, 20 μm.

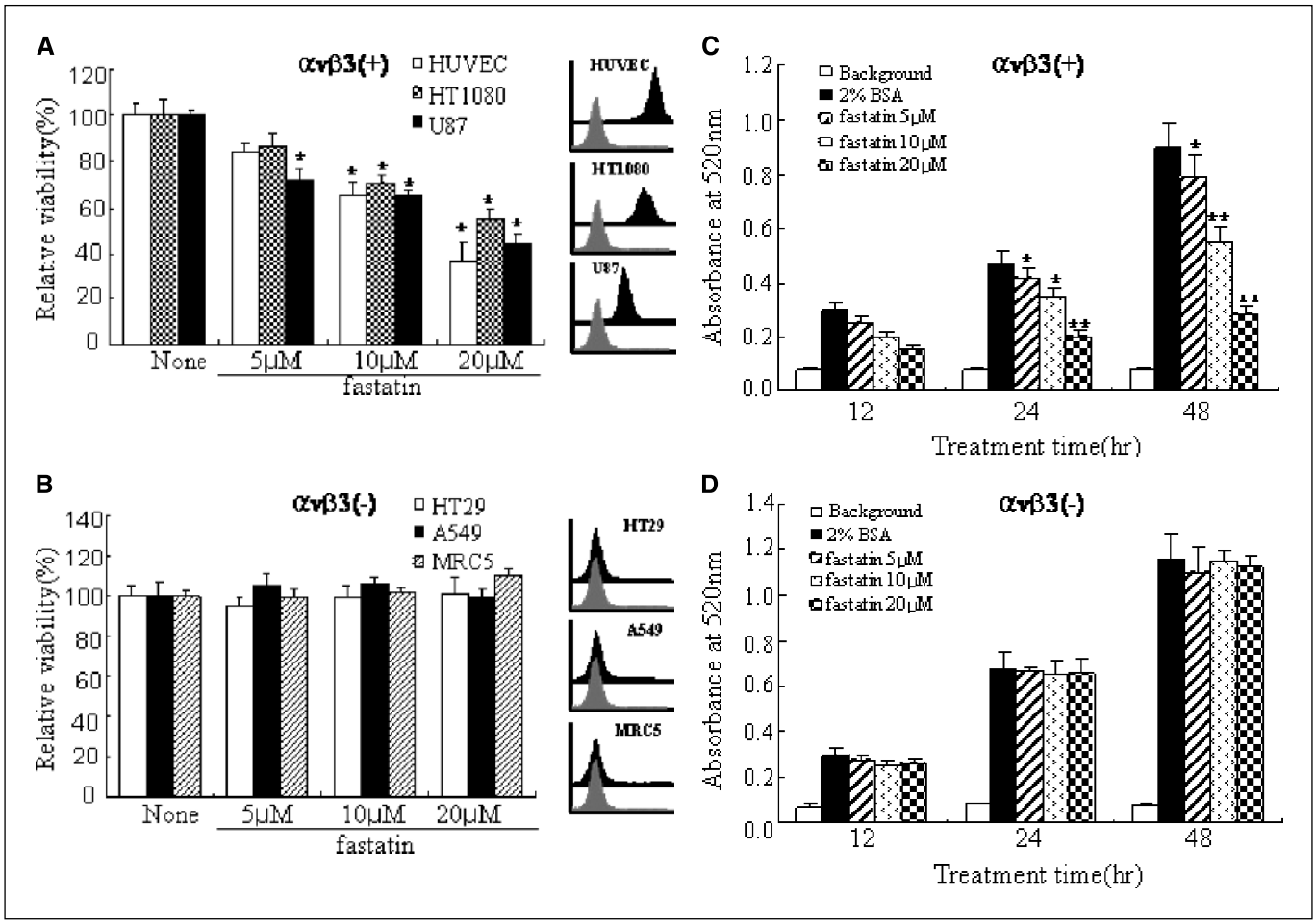

Figure 6. Fastatin inhibits endothelial cell proliferation via αvβ3 integrin. *A-B,* means of three determinations by the MTT assay. Cells were incubated in the presence of indicating concentration of fastatin for 48 hours. Fastatin significantly inhibits the growth of αvβ3 integrin-positive cell lines (HUVEC, HT1080, and U87) but not αvβ3 integrin-negative cell lines (HT29, A549, and MRC5). *C-D,* HUVEC and MRC5 cells were incubated in the presence of increasing concentration of fastatin for up to 12, 24, or 48 hours and a BrdUrd incorporation assay was carried out. *Inset* in *A-B,* analysis of integrins expressed on the cells surface. Flow cytometric analysis was done on cells (*black peak*) stained with saturating concentration of the following monoclonal antibodies: αvβ3 (LM609). Cell number (*y-axis*) plotted as a function of fluorescence intensity (*x-axis*). Representative of three separate experiments. Negative control cells (*gray peak*) were incubated with the secondary antibody alone. *Columns,* means of triplicate wells; *bars,* ±SE. These experiments were repeated thrice. **, $P < 0.01$; *, $P < 0.05$.

(Fig. 6*C-D*). Interestingly, our fluorescence-activated cell sorting analyses disclose that the former cell lines express αvβ3 whereas latter cell lines do not (refs. 17, 18; Fig. 6*A-B*, *inset*), suggesting that this integrin plays a key role in fastatin-mediated cell growth inhibition. Next, we determined whether fastatin induces apoptosis. Fastatin treatment induced a distinct shift in annexin fluorescence intensity in HUVEC cells but not HT29 (Fig. 7*A*). The shift in fluorescence intensity was similar to that of the positive control, TNF-α, in HUVEC. In addition, fastatin increased caspase 3 activity in a dose-dependent manner, which was substantially blocked by DEVD-CHO (Fig. 7*B*). To further confirm whether fastatin mediates the apoptosis via αvβ3 integrin, we employed HEK293 cells stably transfected with a human β3 integrin expression vector. After 48 hours of fastatin treatment, β3/293 cells displayed a distinct shift in the annexin fluorescence peak, in contrast to pc/293 cells stably transfected with empty vector (Fig. 7*C*).

Inhibitory effect of fastatin on signal transduction pathways in endothelial cells. In endothelial cells, FAK, which serves as a platform for different downstream signals, is phosphorylated upon ligand binding to integrins (19). Fastatin inhibited the phosphorylation of FAK when endothelial cells were plated on collagen (Fig. 8*A*). Protein kinase B (PKB/Akt), extracellular signaling-related kinase (ERK), and Raf downstream of FAK play important roles in the regulation of endothelial cell survival, proliferation, and migration (14). Akt additionally regulates protein synthesis by mediating the phosphoryation of eukaryotic initiation factor, 4E-BP1, via mTOR kinase (19). Fastatin inhibited the sustained phosphorylation of Raf, ERK1/2, Akt, and mTOR in HUVEC (Fig. 8*A*). We examined whether these effects of fastatin are αvβ3 integrin dependent. Fastatin treatment resulted in the inhibition of phosphorylation of FAK, Raf, ERK1/2, Akt, and mTOR in β3/293 cells but not pc/293 cells (Fig. 8*B*).

Discussion

In the present study, we show that the FAS1 domain functions as an endogenous regulator of pathogenic angiogenesis, dependent on αvβ3 integrin. The FAS1 domain is present in four human proteins, βig-h3, periostin, FEEL1, and FEEL2. The first two are secretory proteins and the latter two are membranous proteins. We previously reported that the FAS1 domain bears a motif, which interacts with αvβ3 integrin, and that an 18-amino-acid peptide containing this motif displays antiangiogenic activity (13). However, this 18-residue

peptide is a minimal fragment for activity and may not be structurally complete to optimally perform antiangiogenic activity, compared with the FAS1 domain. Fastatin, the fourth FAS1 domain of βig-h3, shows more potent antiangiogenic activity in terms of inhibiting endothelial cell adhesion and migration, as well as *in vitro* and *in vivo*. Interestingly, the domain additionally inhibits endothelial cell adhesion and migration to fibronectin with the RGD-dependent receptor, α5β1 integrin, with similar inhibitory activity, compared with βig-h3 and vitronectin. We previously showed that fastatin-mediated endothelial cell adhesion and migration is RGD-dependent (13). Fastatin cannot efficiently inhibit endothelial cell adhesion and migration to collagen with RGD-independent receptor integrins. Because α5β1 and αvβ3 are important for tumor angiogenesis (14), we assume that fastatin inhibits tumor angiogenesis by blocking both integrins. FAS1 domains of all four human proteins contain the motif for αvβ3 integrin. Accordingly, we hypothesize that any FAS1 domain from the four human proteins potentially has antiangiogenic activity. The second FAS1 domain of βig-h3 and two FAS1 domains of FEEL2 display similar antiangiogenic activities, supporting our hypothesis. Our data additionally show that fastatin results in significant suppression of tumor growth as well as tumor angiogenesis in a mouse tumor model. We employed B16F10 melanoma cells for use in an *in vivo* tumor model. These cells do not express αvβ3 integrin and thus their growth in cultures is not inhibited by fastatin. Overexpression of fastatin in B16F10 cells does not affect cell growth *in vitro* but inhibits tumor growth *in vivo*. Therefore, the antitumorigenic effect of fastatin is possibly not due to direct suppression of tumor cell growth, but inhibition of angiogenesis.

In addition to mediating endothelial cell adhesion and migration, αvβ3 integrin supports endothelial cell growth and survival (20). We have shown that fastatin treatment causes inhibition of endothelial cell growth and induces apoptosis. However, inhibition of growth by fastatin is not restricted to endothelial cells. Interestingly, only αvβ3 integrin-expressing cells are responsive to fastatin. Thus, the inhibition of cell growth and induction of apoptosis by fastatin seem dependent on αvβ3 integrin. This finding is confirmed by experiments using the HEK293 cell line (lacking αvβ3 integrin) stably transfected with αvβ3 integrin. Growth inhibition and apoptosis in response to fastatin are observed only in HEK293 cells expressing αvβ3 integrin. These results are inconsistent with those obtained using the well-studied angiogenesis inhibitor, tumstatin, which also interacts with αvβ3 integrin (21). Growth inhibition by tumstatin is specific to endothelial cells. Tumstatin does not inhibit the growth of other cells, even those expressing αvβ3 integrin on their cell surfaces (19, 21). These data indicate that αvβ3 integrin is essential but not sufficient for tumstatin activity. Further studies are thus required to identify the αvβ3 integrin-associated factors determining the endothelial cell specificity of tumstatin. In contrast, binding of fastatin to αvβ3 integrin is RGD dependent and its inhibition of cell growth is sufficiently mediated via αvβ3 integrin, suggesting that mechanisms of fastatin are distinct from those of tumstatin, although they share the same receptor and some signal pathways.

In endothelial cells, ligand binding to integrins induces the phosphorylation of several signal transducers, including FAK, which

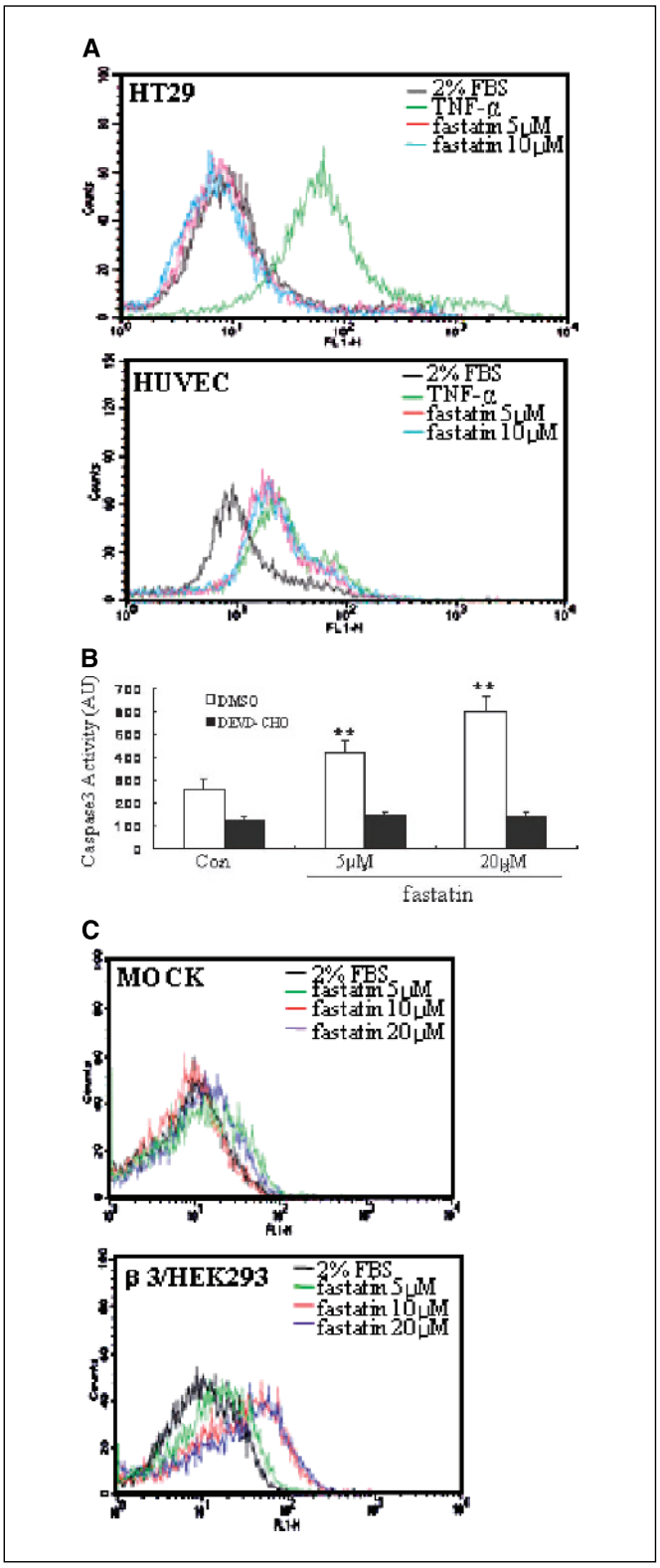

Figure 7. Fastatin induces endothelial cell apoptosis via αvβ3 integrin. *A,* FITC-Annexin V staining. HT29 and HUVEC cells were treated for 48 hours with 5 and 10 μmol/L fastatin (*red* and *sky blue peaks*, respectively), 0.04 μg/mL TNF-α (*green peak*), or an equal volume of PBS (*black peak*). *B,* control and fastatin-treated cells were lysed, and caspase-3 activity was detected. Fastatin increased caspase-3 activity in a dose-dependent manner. In the presence of a specific inhibitor of caspase-3, DEVD-CHO, activity was reduced to the basal level in all groups. *Columns,* means of triplicate wells; *bars,* ±SE. The experiment was repeated thrice. *C,* FITC-Annexin V staining. MOCK and β3/HEK293 cells were treated for 48 hours with 5 to 20 μmol/L fastatin (*yellow green*, *red*, *violet peaks*) or an equal volume of PBS (*black peak*). **, $P < 0.01$.

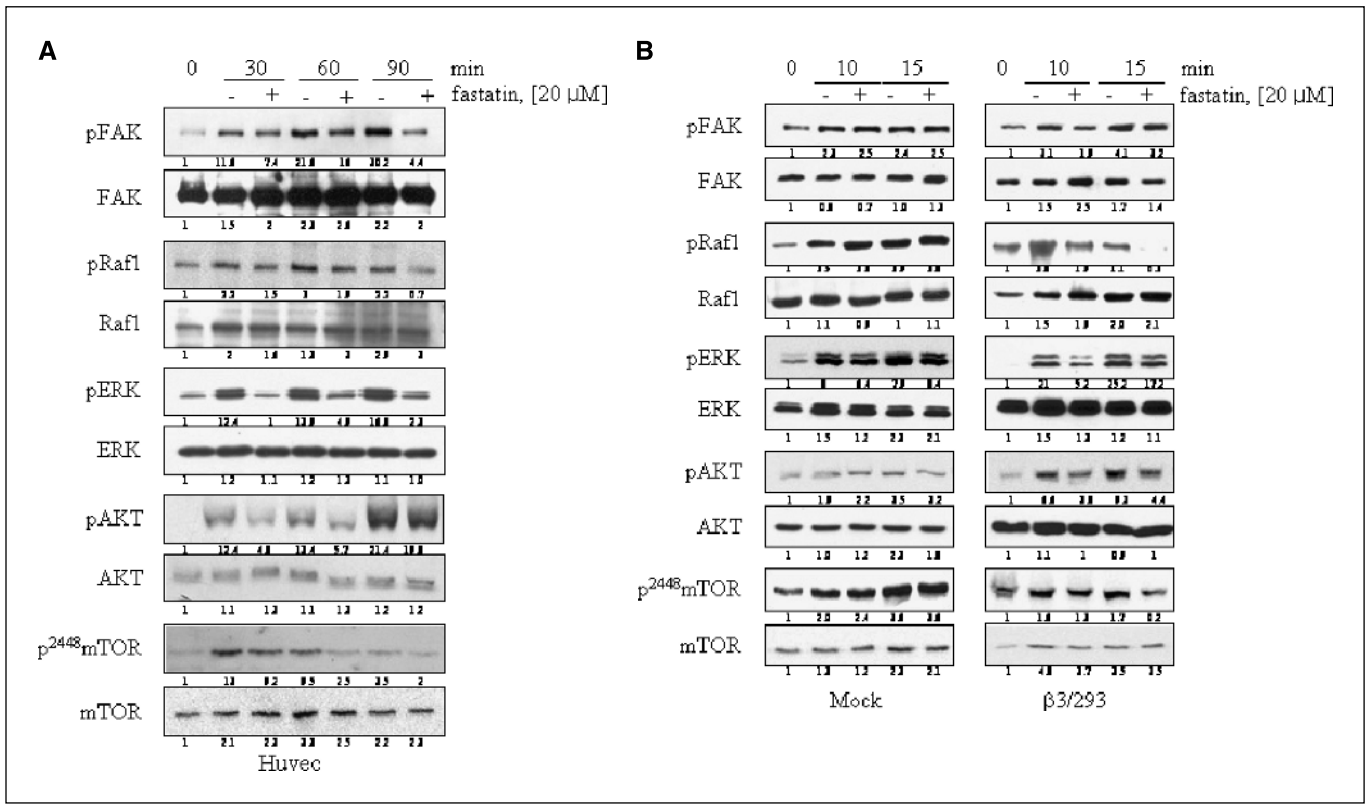

Figure 8. Effects of fastatin on the FAK/Raf/ERK/Akt/mTOR pathway. *A-B,* serum-starved HUVEC, MOCK, and β3/HEK293 cells were plated on collagen-coated dishes in incomplete medium supplemented with fastatin (20 μmol/L) for the indicated times, and lysates analyzed by Western blot using antibodies against the indicated protein (*p,* antibody specific for phosphorylated protein).

serves as a platform for different downstream signals (14, 22). In this study, we show that binding of fastatin to αvβ3 integrin blocks FAK phosphorylation, leading to the inhibition of two main cascades, the Akt/mTOR and Raf/ERK pathways. The Akt/mTOR pathway mediates tumstatin-induced endothelial cell apoptosis via αvβ3 integrin, whereas the Raf/ERK pathway is responsible for the inhibitory effect of endostatin on endothelial migration via α5β1 integrin (14) as well as an αv integrin-mediated angiogenic mechanism in response to basic fibroblast growth factor and vascular endothelial growth factor (VEGF; ref. 21). Fastatin is the first endogenous angiogenesis regulator identified that inhibits both endothelial cell migration and growth by blocking two signal cascades, Akt/mTOR and Raf/ERK pathways elicited by integrin activation. Many of the integrin-induced signaling pathways can also be activated by binding of soluble growth factors to their receptors, which suggests the existence of coordinate mechanisms between integrins and growth factors in the control of cellular functions. In fact, αvβ3 integrin and its downstream mediators are involved in the activation of VEGF (23, 24). Therefore, fastatin could also regulate VEGF-mediated angiogenesis by blocking signal pathways, which are commonly involved in αvβ3 integrin and VEGF.

Both secretory proteins, βig-h3 and periostin, are detected in the circulation. The blood concentration of βig-h3[1] and periostin (25) are about 300 and 962 ng/mL, respectively. The organs or cells that are the main sources of these blood proteins are currently unclear. These may include the liver for the systemic production or platelets or macrophages for local production. Activated platelets and macrophages produce βig-h3 (data not shown), which contributes to form the tumor microenvironment (26). It is also possible that alternative forms or degradation products of FEEL-1 and FEEL-2 are circulated. Notably, HARE (another name for FEEL-2) is cleaved to release a fragment consisting of several FAS1 domains, which presumably circulates in blood (27). In addition, FEEL-1 plays a role in angiogenesis (28). However, it is unclear in which physiologic/pathologic circumstances FAS1 domains such as fastatin are cleaved from FAS1 family proteins and it is also unidentified which protease are responsible for the cleavage of FAS1 proteins. Nevertheless, it would be of interest to determine whether the blood levels of these molecules can be altered, such as thrombospondin (29) and endostatin (30) in tumor patients and in response to antitumor therapy. If this is the case, these domains would be useful biomarkers for antiangiotherapy.

In conclusion, we provide preliminary evidence that FAS1 domains act as endogenous regulators of pathologic angiogenesis, supporting their development as inhibitors for the control of tumor angiogenesis.

[1] Unpublished data.

Acknowledgments

Received 8/2/2004; revised 2/1/2005; accepted 2/8/2005.

Grant support: National Research Laboratory, Korea grant M1010400036-01J0000-01610.

The costs of publication of this article were defrayed in part by the payment of page charges. This article must therefore be hereby marked *advertisement* in accordance with 18 U.S.C. Section 1734 solely to indicate this fact.

We thank Dr. Jeffrey Smith (Burnham Institute, San Diego, CA) for providing the β3/293 cells.

References

1. Skonier J, Neubauer M, Madisen L, Bennett K, Plowman GD, Purchio AF. cDNA cloning and sequence analysis of β ig-h3, a novel gene induced in a human adenocarcinoma cell line after treatment with transforming growth factor-β. DNA Cell Biol 1992;11:511–22.
2. Skonier J, Bennett K, Rothwell V, et al. βig-h3: a transforming growth factor-β-responsive gene encoding a secreted protein that inhibits cell attachment *in vitro* and suppresses the growth of CHO cells in nude mice. DNA Cell Biol 1994;13:571–84.
3. Kim JE, Kim EH, Han EH, et al. A TGF-β-inducible cell adhesion molecule, βig-h3, is downregulated in melorheostosis and involved in osteogenesis. J Cell Biochem 2000;77:169–78.
4. Bae JS, Lee SH, Kim JE, et al. βig-h3 supports keratinocyte adhesion, migration, and proliferation through α3β1 integrin. Biochem Biophys Res Commun 2002;294:940–8.
5. Kim JE, Kim SJ, Jeong HW, et al. RGD peptides released from β ig-h3, a TGF-β-induced cell-adhesive molecule, mediate apoptosis. Oncogene 2003;22:2045–53.
6. Munier FL, Korvatska E, Djemai A, et al. Keratoepithelin mutations in four 5q31-linked corneal dystrophies. Nat Genet 1997;15:247–51.
7. O'Brien ER, Bennett KL, Garvin MR, et al. βig-h3, a transforming growth factor-β-inducible gene, is overexpressed in atherosclerotic and restenotic human vascular lesions. Arterioscler Thromb Vasc Biol 1996; 16:576–84.
8. Lee SH, Bae JS, Park SH, et al. Expression of TGF-β-induced matrix protein βig-h3 is up-regulated in the diabetic rat kidney and human proximal tubular epithelial cells treated with high glucose. Kidney Int 2003;64:1012–21.
9. Park SW, Bae JS, Kim KS, et al. βig-h3 promotes renal proximal tubular epithelial cell adhesion, migration and proliferation through the interactionwith α3β1 integrin. Exp Mol Med 2004;36:211–9.
10. Kawamoto T, Noshiro M, Shen M, et al. Structural and phylogenetic analyses of RGD-CAP/βig-h3, a fasciclin-like adhesion protein expressed in chick chondrocytes. Biochim Biophys Acta 1998;1395:288–92.
11. Kim JE, Kim SJ, Lee BH, Park RW, Kim KS, Kim IS. Identification of motifs for cell adhesion within the repeated domains of transforming growth factor-β-induced gene, βig-h3. J Biol Chem 2000;275:30907–15.
12. Kim JE, Jeong HW, Nam JO, et al. Identification of motifs in the fasciclin domains of the transforming growth factor-β-induced matrix protein βig-h3 that interact with the αvβ5 integrin. J Biol Chem 2002; 277:46159–65.
13. Nam JO, Kim JE, Jeong HW, et al. Identification of the αvβ3 integrin-interacting motif of βig-h3 and its antiangiogenic effect. J Biol Chem 2003;278:25902–9.
14. Sudhakar A, Sugimoto H, Yang C, Lively J, Zeisberg M, Kalluri R. Human tumstatin and human endostatin exhibit distinct antiangiogenic activities mediated by αvβ3 and α5β1 integrins. Proc Natl Acad Sci U S A 2003;100:4766–71.
15. Landegren U. Measurement of cell numbers by means of the endogenous enzyme hexosaminidase. Applications to detection of lymphokines and cell surface antigens. J Immunol Methods 1984;67:379–88.
16. Kwon KB, Park EK, Ryu DG, Park BH. D4-GDI is cleaved by caspase-3 during daunorubicin-induced apoptosis in HL-60 cells. Exp Mol Med 2002;34:32–7.
17. Kunath K, Merdan T, Hegener O, Haberlein H, Kissel T. Integrin targeting using RGD PEI conjugates for *in vitro* gene transfer. J Gene Med 2003;5:558–99.
18. Hamada JI, Omatsu T, Okada F, et al. Overexpression of homeobox gene HOXD3 induces coordinate expression of metastasis-related genes in human lung cancer cells. Int J Cancer 2001;93:516–25.
19. Maeshima Y, Sudhakar A, Lively JC, et al. Tumstatin, an endothelial cell-specific inhibitor of protein synthesis. Science 2002;295:140–3.
20. Brooks PC, Montgomery AM, Rosenfeld M, et al. Integrin α v β 3 antagonists promote tumor regression by inducing apoptosis of angiogenic blood vessels. Cell 1994;79:1157–64.
21. Maeshima Y, Yerramalla UL, Dhanabal M, et al. Extracellular matrix-derived peptide binds to α(v)β(3) integrin and inhibits angiogenesis. J Biol Chem 2001;276:31959–68.
22. Hood JD, Frausto R, Kiosses WB, Schwartz MA, Cheresh DA. Differential αv integrin-mediated Ras-ERK signaling during two pathways of angiogenesis. J Cell Biol 2003;162:933–43.
23. Soldi R, Mitola S, Strasly M, Defilippi P, Tarone G, Bussolino F. Role of αvβ3 integrin in the activation of vascular endothelial growth factor receptor-2. EMBO J 1999;18:882–92.
24. Borges E, Jan Y, Ruoslahti E. Platelet-derived growth factor receptor β and vascular endothelial growth factor receptor 2 bind to the β 3 integrin through its extracellular domain. J Biol Chem 2000; 275:39867–73.
25. Sasaki H, Dai M, Auclair D, et al. Serum level of the periostin, a homologue of an insect cell adhesion molecule, as a prognostic marker in nonsmall cell lung carcinomas. Cancer 2001;92:843–8.
26. Coussens LM, Werb Z. Inflammation and cancer. Nature 2002;420:860–7.
27. Zhou B, Weigel JA, Saxena A, Weigel PH. Molecular cloning and functional expression of the rat 175-kDa hyaluronan receptor for endocytosis. Mol Biol Cell 2002;13:2853–68.
28. Adachi H, Tsujimoto M. FEEL-1, a novel scavenger receptor with *in vitro* bacteria-binding and angiogenesis-modulating activities. J Biol Chem 2002;277: 34264–70.
29. Bocci G, Francia G, Man S, Lawler J, Kerbel RS. Thrombospondin 1, a mediator of the antiangiogenic effects of low-dose metronomic chemotherapy. Proc Natl Acad Sci U S A 2003;100:12917–22.
30. Dhar DK, Ono T, Yamanoi A, et al. Serum endostatin predicts tumor vascularity in hepatocellular carcinoma. Cancer 2002;95:2188–95.

Regulation of Tumor Angiogenesis by Fastatin, the Fourth FAS1 Domain of βig-h3, via αvβ3 Integrin

Ju-Ock Nam, Ha-Won Jeong, Byung-Heon Lee, et al.

Cancer Res 2005;65:4153-4161.